



Lead toxicity in the bald eagle population of the Great Lakes region

Christine Brasic^a, Latimer Harris-Ward^b, Fabio A. Milner^c,
Carlos Bustamante-Orellana^d, Jordy Cevallos-Chavez^d, and Leon Arriola^{d,e}

^aSchool of Mathematics, University of Minnesota-Twin Cities, Minneapolis, USA; ^bDepartment of Physics, University of the Pacific, Stockton, California, USA; ^cSchool of Mathematical and Statistical Sciences, Arizona State University, Tempe, USA; ^dSchool of Human Evolution and Social Change, Arizona State University, Tempe, USA; ^eDepartment of Mathematics, University of Wisconsin-Whitewater, USA

ABSTRACT

Ingestion of lead-based ammunition is one of the leading causes of the mortality of bald eagles. Their primary source is unretrieved carrion contaminated with lead from hunters' ammunition. Lead toxicity can have serious clinical consequences, including reduced fertility and consumption. A model with ordinary differential equations describes the dynamics of available contaminated carrion and the progression of eagles through stages of lead poisoning. Nonnegative solutions exist and equilibrium points are stable for certain parameter ranges. Sensitivity analysis shows that the bald eagle population in the Great Lakes region is primarily dependent on the rate of entry of contaminated carrion in the environment, more so than on retrieval or on the rate of treatment of eagles. Estimates of financial costs of each of these three measures show that the most effective measure is to find a substitute for lead cartridges.

KEYWORDS

Bald eagle population dynamics; differential equations model; ecological forecasting; lead toxicity

1. Introduction

Bald eagles *Haliaeetus leucocephalus* live in Canada, the United States, and Mexico. A 2017 survey by the Wisconsin Department of Natural Resources (Woodford et al., 2017) found 526 occupied nesting territories in Wisconsin's Northern Highland Ecological landscape. The Great Lakes region of the Midwestern United States contains some of the densest bald eagle nesting territories in North America (Woodford et al., 2017).

Apex predators, such as bald eagles, affect ecosystems both directly and indirectly through trophic levels. The mesopredator release hypothesis explains the ecological phenomenon of increasing populations of mesopredators—such as foxes and coyotes—in the absence of apex predators (Estes et al., 2011). This population shift may increase predation of small vertebrate species, or, as in the case of the Yellowstone National Park, reduce predation of

CONTACT Fabio A. Milner  milner@asu.edu  School of Mathematical and Statistical Sciences, Arizona State University, P.O. Box 871804, Tempe, AZ 85287 USA.

This article has been corrected with minor changes. These changes do not impact the academic content of the article.
© 2021 Taylor & Francis

elk (*Cervus canadensis*), resulting in overgrazing of plant life (Farquhar, 2020). In the *Encyclopedia of Biodiversity*, Estes et al. (2001: 864) wrote that “freshwater lakes provide the best known evidence for trophic cascades [...] lake systems throughout the world show altered populations of apex predators resulted in altered food webs” and describe phytoplankton, herbivores, zooplankton-eating predators, and fish-eating predators as the essential organism groups in lake ecosystems. Bunnell et al. (2013) described top-down trophic cascades in the Great Lakes, beginning with decreases in native top predators eating lake trout (*Salvelinus namaycush*) through overfishing and the introduction of parasitic sea lamprey (*Petromyzon marinus*). Increasing the alewife (*Alosa pseudoharengus*) population gave rise to small zooplankton species, due to alewife preferring large zooplankton prey. These alterations in the food web, along with accumulating pollution, eventually led to the lake eutrophication in the 1970s. Harvey et al. (2012) simulated the top-down influence of both resident and overwintering bald eagles in a marine ecosystem to show that bald eagles are “capable of influencing community structure through direct and indirect trophic effects” (: 907). Bald eagles help maintain ecological stability through their interactions as apex predators with other species of the Great Lakes ecosystem.

Lodenius and Solonen (2013) evaluated the contamination of the environment of predatory birds. Kramer and Redig (1997), comparing lead toxicity in bald eagles admitted to the University of Minnesota Raptor Center between 1980 and 1995, before and after state and federal bans of lead ammunition in waterfowl hunting, reported that changes in prevalence of lead-exposed or poisoned eagles are not statistically significant. Eagles submitted before the bans “were more acutely affected and lead poisoning was indicated [...] as the primary cause of admission” (: 331). After the bans, they found trauma as the main reason for admission with blood lead levels suggesting chronic lead exposure.

Eagles with serum lead levels under 0.2 ppm (part per million) are considered lead free, as these levels are considered background; eagles with serum lead levels between 0.2 and 0.5 ppm are classified as having subclinical lead toxicity; eagles with serum lead levels over 0.5 ppm are classified as having clinical lead toxicity (Golden et al., 2016). We also model the subtle, long-term damage of eagles with subclinical lead toxicity (Redig et al., 2007b; Hunt, 2012) through a reduction in fertility and voracity. Due to the severity of clinical lead toxicity (Redig et al., 2007a; Russell and Franson, 2014), eagles with clinical lead toxicity, which is the final stage of lead toxicity, either succumb to lead poisoning or are retrieved and given therapy and rehabilitation. Hence, we assume that all additional mortality of eagles is due to clinical lead toxicity or failure of clinical lead toxicity treatment. Eagles with clinical lead toxicity do not reproduce, and we assume that they no longer accumulate lead from further consumption of contaminated carrion.

Hallam et al. (1983) used differential equations governing the population biomass, the concentration of toxicant in an organism, and the concentration of toxicant in the environment, coupled by a linear dose-response function, to model the effect of a toxicant on a population. Cruz-Martinez et al. (2012) and Kramer and Redig (1997) represented bald eagles feeding on lead-contaminated offal and unretrieved game during firearm hunting seasons but ignored that lead accumulates in the environment.

No one has examined the effects of lead toxicity on the population dynamics of the bald eagle. This is the gap we address.

We shall forecast that, at the current rate of winter food-source contamination, the bald eagle population would reach 36,000 individuals at the end of a 25-year period. Removing the source of contamination would lead to an increase of 1.2% in their total number. In contrast, changing the rate at which wildlife rehabilitation centers retrieve bald eagles for treatment would only increase their population by 0.07% during the same period of time.

2. Method

2.1. Data

We consider the eight States that surround the Great Lakes of the United States: Illinois, Iowa, Indiana, Michigan, Minnesota, Missouri, Ohio, and Wisconsin. North central Wisconsin has “one of the highest densities of nesting bald eagles anywhere in North America,” with 550 occupied nests, which represent 32.7% of the 1,684 occupied nests in the survey covering seven areas (Magana et al., 2019). Although most bald eagles live in the northern States, eagles migrate and spend winters in States to the south (Shepherd, 2019). Consequently, we include States to the south of the Great Lakes because lead toxicity levels and lead accumulation during the winter are correlated with one another (Neumann, 2009; Russell and Franson, 2014; Lindblom et al., 2017; Simon et al., 2020).

We estimated the total number of occupied bald eagle nests using data from the United States Fish and Wildlife Service, the State Departments of Natural Resources, and the Center for Biological Diversity (Suckling and Hodges, 2007; U.S. Fish and Wildlife Service, 2016; Magana et al., 2019; Indiana Department of Natural Resources, 2020; U.S. Fish and Wildlife Service Midwest Region, 2020a). Magana et al. (2019) identified occupied nests inhabited by either an incubating adult, eggs, young eaglets, or those being repaired. According to the United States Fish and Wildlife Service 2016, bald eagles over the age of 4 years constitute 43% of the population and couples of adult eagles occupy nests. We estimate the total population size as

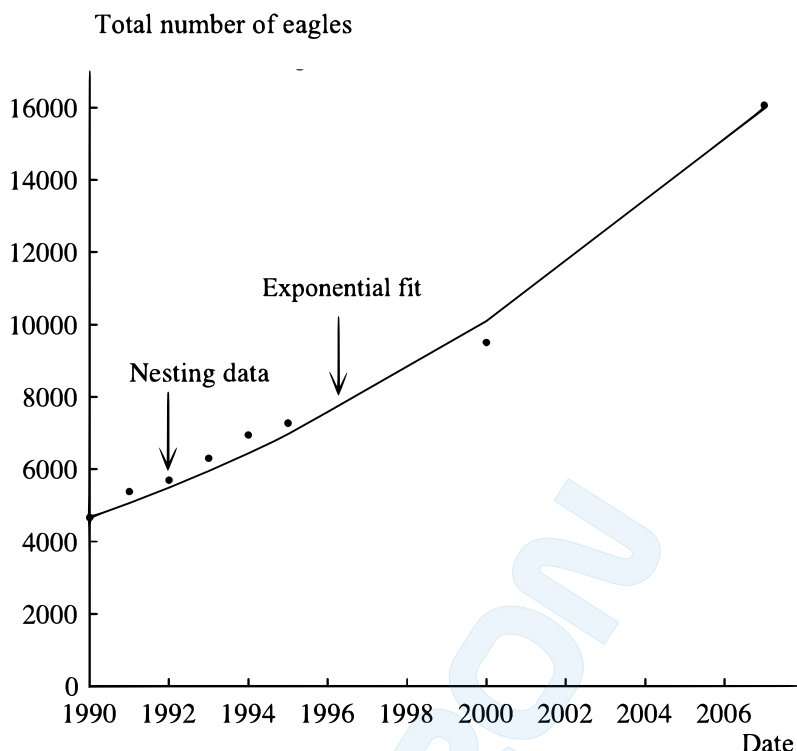


Figure 1. Exponential fit of the bald eagle data in the Great Lakes region from 1990 to 2007.

$$\text{total population size} = \frac{2}{0.43} \times (\text{total number of occupied nests}). \quad (1)$$

Figure 1 shows the fit of the total bald eagle population data for the Great Lakes region from 1990 to 2007—summarized in Table 1, built using Eq. (1)—to an exponential curve. However, because we wish to explore the model outside the empirical values specific to the eagle population of the Great Lakes, we consider this exponential as the beginning of a logistic curve, which leads us to introduce the carrying capacity as a parameter.

Table 1. Occupied nesting territories in the Great Lakes region.

Year	Total number of occupied nesting territories	Total population size
1990	1003	4665
1991	1157	5381
1992	1225	5697
1993	1355	6302
1994	1494	6948
1995	1564	7274
2000	2044	9506
2007	3454	16065
2009	5879	27344

2.2. Background and assumptions

Based on 58 bald eagle carcasses from Iowa, Minnesota, and Wisconsin, Warner et al. (2014) found “no significant difference in liver lead concentrations between [male and female eagles]” (: 211). Franson and Russell (2014) diagnosed that female eagles were more intoxicated with lead than males (: 1728). For 484 bald and 68 golden eagles diagnosed with lead poisoning, they concluded that “more than half were characterized as being in emaciated or poor body condition, suggesting that most were undergoing chronic poisoning and not obtaining adequate nutrition” (: 1728). Warner et al. (2014) obtained a “significant negative correlation between liver lead and body mass for eagle carcasses from the Upper Midwest” (: 211). Franson and Russell (2014) found 14.2% bald eagles with lead in their stomachs. Likewise, Neumann (2009) reported from x-ray analysis of lead-poisoned bald eagles in Iowa that 11.8% have lead remaining in their digestive tracts. Cruz-Martinez et al. (2012) also found that 11% of bald eagles “had radiographic evidence of metallic foreign objects in their gastro-intestinal tracts” (: 98). However, Stauber et al. (2010) found no evidence of lead in the digestive tracts of 67 eagles tested between 1991 and 2008 in the Pacific Northwest.

Fallon et al. (2017) provided guidelines for evaluation and treatment, suggesting that birds whose blood-lead levels are under 40 mg/dl be released back to the wild as soon as possible after capture, while the release or treatment of birds with blood-lead levels between 40 mg/dl and 60 mg/dl should be made based on the presence of clinical signs of poisoning and relevant biological characteristics (for example, breeding status). Birds with blood-lead levels higher than 60 mg/dl are potentially lethally poisoned and should be removed from the wild for appropriate treatment and later release.

We only consider lead among anthropogenic factors affecting bald eagles. Bald eagles scavenge during the big-game hunting seasons (Neumann, 2009; National Eagle Center, 2020) and several studies suggest a strong association between lead-based ammunition, hunting seasons, and lead toxicity in scavenging species. Stauber et al. (2010) reported higher prevalence of lead in blood of eagles submitted to the Washington State University Raptor Rehabilitation program corresponding to local firearm hunting seasons and inland migration of eagles during winter. Warner et al. (2014), based on radiographic imaging of offal piles from deer shot with lead ammunition, found that both shotguns and muzzleloader rifles produce lead fragments in offal piles (: 211).

Cruz-Martinez et al. (2012), based on data of high lead levels in bald eagles from Minnesota, Wisconsin, and Iowa, reported eagle location by State as not a significant factor, month of admission as significant, with the most significant months being November, December, and January, and the highest odds during December, January, February, and March in eagles recovered from the rifle zone and in adult individuals. Kramer and

Redig (1997) also found the highest rates of eagle admission in November and December, which correspond to the deer season in Minnesota and Wisconsin.

Based on these, we assume that eagles acquire lead toxicity through the consumption of lead-contaminated carrion. We divide the population into four disjoint compartments: lead-free eagles, those with one of two stages of lead toxicity, and those under treatment for lead toxicity. If treatment of clinical lead toxicity is successful, these eagles retain lasting physiological damage (Fallon et al., 2017) and, in the model, return to the compartment of subclinical lead toxicity rather than to that of lead-free eagles.

Lead binds to calcium, settling in the bones of eagles over time (Hunt, 2012). Lead accumulated within the bones remains stable for long periods of time, but during egg formation may remobilize into the bloodstream, accumulating in eggshells, and in newborn eaglets (Burger, 1994; Gangoso et al., 2009; Vallverdú-Coll et al., 2015; Bruggeman et al., 2018; Gil-Sánchez et al., 2018). Therefore, we assume that eagles transfer their lead toxicity to their offspring. We also assume that the eagle population is not affected by migration and that it grows logistically in the absence of lead.

2.3. Model formulation

(1) Contaminated carrion: total mass $C(t)$ at time t

We assume that contaminated carrion increases at the constant annual rate Λ and that it is the only source of lead for bald eagles. The rate Λ represents the annual amount of unretrieved game containing fragments of spent lead ammunition. Eagles may also scavenge uncontaminated carrion; the percentage of carrion that is $C(t)$ divided by the constant total mass M of available carrion. Carrion also decreases at the rate μ_1 from natural decomposition. These assumptions lead to the dynamic of $C(t)$:

$$C'(t) = \Lambda - \frac{\delta_1}{M} C(t)S(t) - \frac{\omega\delta_1}{M} C(t)L(t) - \mu_1 C(t). \quad (2)$$

(2) Lead-free eagles: total number $S(t)$ at time t

Lead-free (or uncontaminated) eagles increase in number at rate r . Because these eagles have little to no lead contamination, their fertility is not affected. The total population of eagles in the Great Lakes region is growing logistically with a carrying capacity K , as explained after Figure 1. As lead-free eagles scavenge contaminated carrion, they acquire lead toxicity (Cruz-Martinez

et al., 2012). These eagles acquire subclinical lead toxicity at rate ω_1 , when all available carrion is contaminated with lead. We assume lead-free eagles are otherwise healthy, so they die only by other causes, at mortality rate μ_2 :

$$S'(t) = rS(t) \left(1 - \frac{S(t) + L(t) + H(t) + T(t)}{K} \right) - \frac{\omega_1}{M} C(t)S(t) - \mu_2 S(t). \quad (3)$$

(3) Eagles with subclinical lead toxicity: total number $L(t)$ at time t

Eagles with subclinical lead toxicity have detectable levels of lead in their blood, in the range of 0.2 to 0.5 ppm. They show no clinical symptoms (Golden et al., 2016), but suffer physiological damage and have their appetite reduced by a factor w . Their scavenging rate is $w\delta_1$, where $0 < w < 1$, and their fertility in the model is reduced (Redig et al., 2007b; Hunt, 2012) to vr , where $0 < v < 1$. Their offspring are born into the class of subclinical lead toxicity due to maternal transmission of lead (Burger, 1994; Vallverdú-Coll et al., 2015; Bruggeman et al., 2018; Gil-Sánchez et al., 2018). Inflow to the class of subclinical lead toxicity comes both from lead-free eagles, at rate ω_1 , and from eagles leaving treatment, at rate ρ . Eagles leaving treatment suffer lasting damage, as chelation therapy does not clean up their serum lead levels; hence, they return to the class of subclinical lead toxicity rather than to the lead free class (Fallon et al., 2017). The per head outflow rate ω_2 from the subclinical lead toxicity class is less than the individual inflow rate ω_1 into this compartment because subclinical lead toxicity reduces appetite and because the amount of lead to be accumulated to move one eagle into the class of clinical lead toxicity is larger than the amount of lead necessary to move a lead-free eagle into the class of subclinical lead toxicity. Therefore we assume these eagles die from other causes, at mortality rate μ_2 :

$$L'(t) = vrL(t) \left(1 - \frac{S(t) + L(t) + H(t) + T(t)}{K} \right) + \frac{\omega_1}{M} C(t)S(t) + \rho T(t) - \frac{\omega_2}{M} C(t)L(t) - \mu_2 L(t). \quad (4)$$

(4) Eagles with clinical lead toxicity: total number $H(t)$ at time t

Eagles with clinical lead toxicity have serum lead levels high enough (> 0.5 ppm) to show difficulty in flying, gross lesions on organs, or total loss of appetite (Hunt, 2012; Fallon et al., 2017). Eagles with subclinical lead toxicity acquire clinical lead toxicity at rate ω_2 when all available carrion is contaminated with lead. Eagles with clinical lead toxicity die of lead at rate μ_3 and of other causes at rate μ_2 . They may also be retrieved for veterinary care in the treatment class, at rate η . They are too sick to be fertile or to feed (thus they no longer increase their lead levels):

$$H'(t) = \frac{\omega_2}{M} C(t)L(t) - (\eta + \mu_2 + \mu_3) H(t). \quad (5)$$

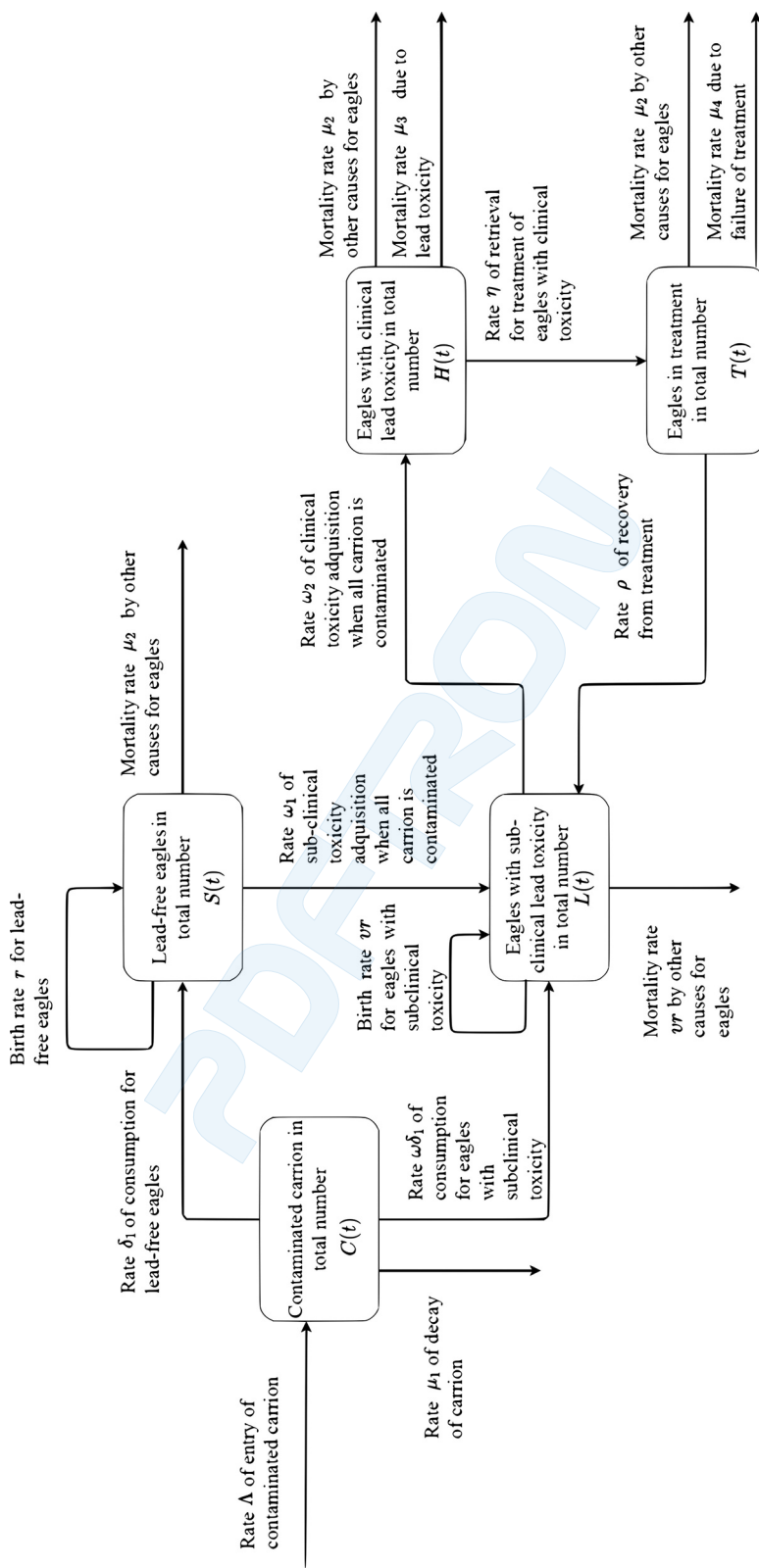


Figure 2. Compartments of the model: at time t , lead-free eagles, in total number $S(t)$, eagles with subclinical lead toxicity, in total number $L(t)$, eagles with clinical lead toxicity, in total number $H(t)$, and eagles in treatment, in total number $T(t)$. Eagles move through each compartment by interacting with the total mass $C(t)$ of contaminated carion.

(5) Eagles in treatment: total number $T(t)$ at time t

The treatment compartment comprises eagles with clinical symptoms of lead toxicity. Humans treat clinically lead-poisoned eagles at rate η . Because chelation therapy involves its own risks (Redig et al., 2007a; Fallon et al., 2017), it is administered until eagles reach a subclinical rather than a background level of lead so that, when released, these eagles are not lead free. Eagles in treatment may be euthanized (at rate μ_4) or die from other causes (at rate μ_2). Eagles surviving the treatment and declared fit are released in the wild (at rate ρ) (Redig et al., 2007a):

$$T'(t) = \eta H(t) - (\rho + \mu_2 + \mu_4)T(t). \quad (6)$$

The total eagle population size at time t is

$$N(t) = S(t) + L(t) + H(t) + T(t). \quad (7)$$

The model is represented as a flow diagram in Figure 2.

2.4. Setting the parameters

We assume that eagles consume lead only through scavenging lead-shot carrion, during the deer-hunting firearm seasons, which are in fall and in winter (Wisconsin Department of Natural Resources, 2017). Combining 2009, 2012, 2013, and 2019 deer harvest reports, we estimate an annual harvest of 900,000 deer (Missouri Department of Conservation, 2012; Watt et al., 2012; Warner et al., 2014). Nixon et al. (2001), Neumann (2009), and Warner et al. (2014) agree that 10% to 32% of the deer that are shot are not retrieved by hunters.

With adding poaching and discarded offal, we assume that 32% of hunted deer go unretrieved, which corresponds to 280,000 deer per year. For an average mass of a deer in Wisconsin of 72 kilograms (Watt et al., 2012), we estimate the total annual mass of carrion M to be 20,000 tons.

We use Freed and Yarbrough's (2008) estimate that 15% of venison donated to Wisconsin food pantries was contaminated with lead. We assume that the proportion of unretrieved deer is the same, which corresponds to an entry rate Λ of contaminated carrion of 3,000 tons per year.

Jennelle et al. (2009) found that a deer carcass in Wisconsin remains in the environment for 18 to 55 days during the fall and winter seasons, which allows us to estimate the natural decay rate of carrion $\mu_1 = 1 \text{ year}^{-1}$. According to the American Eagle Foundation (2020), a bald eagle consumes between 219 and 365 pounds of food annually, which is a consumption rate δ_1 of 132 kg/yr for lead-free eagles. Hunt (2012), Franson and Russell (2014), and Golden et al. (2016) mentioned that lead toxicity reduces consumption, but none of these

authors quantified that. That is why we assume a reduction factor $w = 0.9$, which leads to the per-head consumption rate $w\delta_1$ of eagles with subclinical lead toxicity estimated at 118.8 kilograms per year.

Data from Neumann (2009) for Iowa in the years 2007 and 2008 show a 9.5% increase in the total number of eagles with subclinical lead toxicity, which leads to an estimated rate $\omega_1 = 0.100$ at which lead-free eagles become ill with subclinical lead toxicity when all carrion they ingest is contaminated. Likewise, the annual turnover among eagles with clinical lead toxicity corresponds to a rate of $\omega_2 = 0.142$ at which eagles with subclinical lead toxicity acquire clinical lead toxicity when all carrion is contaminated.

In 2016, the U.S. Fish and Wildlife Service determined the carrying capacity of the bald eagle for the entire United States as 227,800 (U.S. Fish and Wildlife Service, 2016). In 2009 the Great Lakes Region contained 20% of the country's bald eagle population. Thus we assume that the carrying capacity for the bald eagle in the Great Lakes region is 20% of that for the U.S., that is $K = 46,000$ individuals.

The Service also calculated the growth rate in the absence of anthropogenic factors as $r = 0.206$ a year, beginning with 2007. Chronic lead toxicity damages reproductive organs (Redig et al., 2007a; Fallon et al., 2017), but the reduction in fertility has not been quantified. Gil-Sánchez et al. (2018) estimated the fertility reduction factor among Bonelli eagles with subclinical lead toxicity at $v = 0.7$. The treatment rate η of eagles with clinical lead toxicity depends on human intervention. We use $\eta = 4.0$ as the reference value and vary this positive parameter to simulate scenarios ranging from no eagles being retrieved ($\eta = 0$) for treatment to all eagles being retrieved ($\eta \rightarrow \infty$). Because bald eagles begin courtship and nest construction, and mate in the winter (Warner et al., 2014; Shepherd, 2019; U.S. Fish and Wildlife Service Midwest Region, 2020b), we assume that eagles in treatment for clinical lead toxicity do not reproduce.

Chelation therapy and rehabilitation take from weeks to months (Redig et al., 2007a, 2007b; Fallon et al., 2017). Hence, the recovery rate from therapy ρ is set to 1 per year, representing an average duration of treatment of one year. This value allows the eagles to skip the mating season (winter). Over a year, 20% of eagles in treatment are euthanized (Strom et al., 2009; Yaw et al., 2017), corresponding to a mortality rate $\mu_4 = 0.223$.

3. Analysis

We prove now that the model of Eq. (2) to (7) provides nonnegative solutions for all time from any nonnegative initial conditions and that, if the total population size is initially below the carrying capacity, then it stays below it forever. We also characterize equilibria or long-term behavior and, by varying

the rate μ_1 of natural decay and the treatment rate η of eagles with clinical lead toxicity, quantify the effects of the removal of contaminated carrion or the treatment of eagles affected by lead toxicity.

For algebra, we used Mathematica 12.1 (Wolfram Research, Inc., 2020) and Maple 2019 (Maplesoft, a division of Waterloo Maple Inc., 2019); for simulations, we used Matlab R2019a, R2020a (Mathworks, Inc., 2019; Mathworks, Inc., 2020), and R 3.6.1 (R Core Team, 2019). We prepared data using this version of R.

3.1. Positivity of solutions

We prove that when Eq. (2) to (6) have nonnegative initial conditions, they also have nonnegative global solutions. For lead-free eagles in total initial number $S(0) > 0$ and for the rate $\Lambda(t)$ of entry for contaminated carrion a positive constant on the intervals $[n, n + 0.25]$ and zero on the intervals $(n + 0.25, n + 1)$, for all $n \in \mathbb{Z}$, entry of contaminated carrion occurs only during the big-game hunting season, from mid-October to mid-January. We prove that all state variables are strictly positive forever when starting from nonnegative initial conditions.

The existence and uniqueness theorem for ordinary differential equations (Boyce and DiPrima, 2005, Theorem 7.1.1) ensures that a unique solution exists for $t \in [0, +\infty)$. Eq. (2) guarantees that contaminated carrion $C(t)$ is strictly positive for $t > 0$:

$$\text{For } g(t) := \frac{\delta_1}{M} S(t) + \frac{w\delta_1}{M} L(t) + \mu_1, \quad (8)$$

and

$$G(t) = \int_0^t g(s) \, ds, \quad (9)$$

we have

$$C(t) = C(0) \exp(-G(t)) + \Lambda \int_0^t \exp(G(s) - G(t)) \, ds > 0 \quad (10)$$

on the intervals $[n, n + 0.25]$ ($n \in \mathbb{Z}$) because $\Lambda(n) > 0$. $C(t)$ is also strictly positive on the intervals $(n + 0.25, n + 1)$ ($n \in \mathbb{Z}$) because $C(n + 0.25) > 0$ for all $n \in \mathbb{Z}$. Likewise, Eq. (3) guarantees that $S(t)$ is strictly positive for $0 < t < +\infty$:

$$S(t) = S(0) \exp\left(\int_0^t \left(r \left(1 - \frac{S(\tau) + L(\tau) + H(\tau) + T(\tau)}{K}\right) - \frac{\omega_1}{M} C(\tau) - \mu_2\right) d\tau\right) > 0, \quad (11)$$

as $S(0) > 0$.

We prove that

$$L(0), H(0), T(0) \geq 0 \Rightarrow L(t), H(t), T(t) \geq 0 \text{ for } 0 \leq t \leq \varepsilon \quad (12)$$

if $\varepsilon > 0$ is small enough. Assume that $C(0) > 0$ and $S(0) > 0$. The continuity of C, S, L, H , and T , and $T(0) \geq 0$ imply that the term $\frac{\omega_1}{M} C(t)S(t) + \rho T(t)$ in Eq. (4) is strictly positive for $0 \leq t \leq \varepsilon$ if $\varepsilon > 0$ is small enough. For $t \in (0, \varepsilon]$, we use the argument in Eq. (2) applied to Eq. (4) to prove that $L(t) > 0$ and $C(t) > 0$, to Eq. (5) to show that $H(t) > 0$, and to Eq. (6) to show that $T(t) > 0$ on $(0, \varepsilon]$. This establishes the local-in-time conservation of positivity. We now show that this is true globally.

We assume that $C(0) > 0$ and $S(0) > 0$, which implies that $C(t) > 0$ and $S(t) > 0$ for $t \geq 0$. By contradiction, assume that the solution may take negative values. Define $\bar{t} = \inf\{t > 0 : L(t) = 0 \text{ or } H(t) = 0 \text{ or } T(t) = 0\}$. The state variables $L(t), H(t)$, and $T(t)$ are strictly positive on the interval $(0, \bar{t})$ and $\bar{t} \geq \varepsilon > 0$.

Because the term $\frac{\omega_1}{M} C(t)S(t) + \rho T(t)$ in Eq. (4) is strictly positive for $0 \leq t \leq \bar{t}$, there exists a $\varepsilon_1 > 0$ such that it is also strictly positive for $\bar{t} \leq t \leq \bar{t} + \varepsilon_1$. Hence, by Eq. (4), $L(t) > 0$ on $(0, \bar{t} + \varepsilon_1]$ if $\varepsilon_1 > 0$ is small enough.

The term $\frac{\omega_2}{M} C(t)L(t)$ in Eq. (5) is strictly positive on $(0, \bar{t} + \varepsilon_1]$. Hence, by Eq. (5), we deduce that $H(t) > 0$ on $(0, \bar{t} + \varepsilon_1]$. Given that the source term $\eta H(t)$ in Eq. (6) is strictly positive on $(0, \bar{t} + \varepsilon_1]$, it follows from Eq. (6) that $T(t) > 0$ on $(0, \bar{t} + \varepsilon_1]$. There is a contradiction because $L(\bar{t}), H(\bar{t}), T(\bar{t}) > 0$. This proves that, if $C(0) > 0, S(0) > 0, L(0) \geq 0, H(0) \geq 0$, and $T(0) \geq 0$, then $L(t) > 0, H(t) > 0$, and $T(t) > 0$ for $t \geq 0$.

3.2. The population size is upper bounded by $(1 - \frac{\mu_2}{r})K$, if $\mu_2 \leq r$

We sum Eq. (3), (4), (5), and (6) to obtain

$$N'(t) = r(S(t) + \nu L(t)) \left(1 - \frac{N(t)}{K}\right) - \mu_2 N(t) - \mu_3 H(t) - \mu_4 T(t). \quad (13)$$

If $0 < N(0) < (1 - \frac{\mu_2}{r})K$, then $N(t) < (1 - \frac{\mu_2}{r})K$ for all $t \geq 0$. If there is a $t > 0$ such that $N(t) = (1 - \frac{\mu_2}{r})K$, we call \tilde{t} the smallest such time, that is, $N(\tilde{t}) = (1 - \frac{\mu_2}{r})K$, but $N(t) < (1 - \frac{\mu_2}{r})K$ for $[0, \tilde{t})$. From Eq. (13),

$$\begin{aligned} N'(\tilde{t}) &= \mu_2(S(\tilde{t}) + \nu L(\tilde{t})) - \mu_2 \left(1 - \frac{\mu_2}{r}\right)K - \mu_3 H(\tilde{t}) - \mu_4 T(\tilde{t}) < -\mu_3 H(\tilde{t}) \\ &\quad - \mu_4 T(\tilde{t}) < 0. \end{aligned} \quad (14)$$

By continuity, $N'(t)$ is negative on the interval $(\tilde{t} - \varepsilon, \tilde{t})$ on which $N(t) < (1 - \frac{\mu_2}{r})K$, forbidding to have $N(t) = (1 - \frac{\mu_2}{r})K$ for any $t > 0$. The upper bound for the total population size,

$$N_{\sup} = \left(1 - \frac{\mu_2}{r}\right)K, \quad (15)$$

is the *effective carrying capacity*, corresponding to the logistic equation with exponential rate $r - \mu_2$, which is the difference between the birth and mortality rates.

3.3. Steady states

The steady states of System $\{(2), (3), (4), (5), (6)\}$ are the zeros of the system of linear and quadratic equations:

$$\Lambda - \frac{\delta_1}{M} C^* S^* - \frac{w\delta_1}{M} C^* L^* - \mu_1 C^* = 0, \quad (16)$$

$$rS^* \left(1 - \frac{S^* + L^* + H^* + T^*}{K}\right) - \frac{\omega_1}{M} C^* S^* - \mu_2 S^* = 0, \quad (17)$$

$$vrL^* \left(1 - \frac{S^* + L^* + H^* + T^*}{K}\right) + \frac{\omega_1}{M} C^* S^* + \rho T^* - \frac{\omega_2}{M} C^* L^* - \mu_2 L^* = 0, \quad (18)$$

$$\frac{\omega_2}{M} C^* L^* - \sigma_1 H^* = 0, \quad (19)$$

$$\eta H^* - \sigma_2 T^* = 0. \quad (20)$$

The asterisks denote the values at the steady state. We introduce

$$\sigma_1 := \eta + \mu_2 + \mu_3 \quad \text{and} \quad \sigma_2 := \rho + \mu_2 + \mu_4. \quad (21)$$

From Eq. (16), the steady state for the total mass of contaminated carrion is

$$C^* = \frac{\delta_1}{M} (S^* + wL^*) + \frac{\Lambda}{\mu_1}. \quad (22)$$

From Eq. (17), the steady states for the total number of lead-free eagles are

$$S^* = 0 \quad (23)$$

$$\text{and } S^* = \frac{K (r - \frac{\omega_1}{M} C^* - \mu_2)}{r} - (H^* + L^* + T^*). \quad (24)$$

From Eq. (18), (19), and (20), the steady states for the other state variables are

$$L^* = \frac{\frac{\omega_1}{M} C^* S^* + \rho T^*}{\frac{\omega_2}{M} C^* + \mu_2 - vr \left(1 - \frac{S^* + L^* + H^* + T^*}{K}\right)}, \quad (25)$$

$$H^* = \frac{\omega_2}{M} \frac{C^* L^*}{\sigma_1}, \quad (26)$$

$$T^* = \frac{\eta H^*}{\sigma_2}. \quad (27)$$

$L^* = 0$ in Eq. (26) gives $H^* = 0$ and Eq. (27) gives $T^* = 0$. For $L^* = 0$, $H^* = 0$, and $T^* = 0$ in Eq. (18), $C^* S^* = 0$. Then either $C^* = 0$ or $S^* = 0$. If $C^* \neq 0$, then $C^* = \frac{\Lambda}{\mu_1} \geq 0$. At the equilibrium point x_1^* , there are no eagles in any class and the total mass of contaminated carrion is $\frac{\Lambda}{\mu_1}$, that is:

$$x_1^* := (C_1^*, S_1^*, L_1^*, H_1^*, T_1^*) = \left(\frac{\Lambda}{\mu_1}, 0, 0, 0, 0 \right). \quad (28)$$

It corresponds to the rate Λ of entry of contaminated carrion multiplied by its average permanence in the environment in the absence of eagles at every stage of toxicity—the reciprocal of the rate μ_1 of natural decay of contaminated carrion.

In case of no entry of carrion into the environment, $C^* = 0$, there are no eagles with clinical lead toxicity at equilibrium, that is, $H^* = 0$. From Eq. (20), there are no eagles in treatment, that is, $T_2^* = 0$. The system of Eq. (16) to (20) reduces to Eq. (17) and (18), which become

$$rS_2^* \left(1 - \frac{S_2^* + L_2^*}{K} \right) - \mu_2 S_2^* = 0, \quad (29)$$

$$vrL_2^* \left(1 - \frac{S_2^* + L_2^*}{K} \right) - \mu_2 L_2^* = 0. \quad (30)$$

Substituting $S_2^* = \left(\frac{\mu_2}{r} - 1\right)K$ into $L_2^* = \left(\frac{\mu_2}{vr} - 1\right)K$ yields $\frac{\mu_2}{r} = \frac{\mu_2}{vr}$, which implies $v = 1$, which no longer corresponds to a reduction of fertility. In the absence of lead-contaminated carrion, if the total population of eagles $N(t)$ is nonzero, it consists entirely either of lead-free eagles or of eagles with sub-clinical toxicity, giving two equilibrium points:

$$x_2^* := (C_2^*, S_2^*, L_2^*, H_2^*, T_2^*) = \left(0, K \left(1 - \frac{\mu_2}{r} \right), 0, 0, 0 \right),$$

and

$$x_3^* := (C_3^*, S_3^*, L_3^*, H_3^*, T_3^*) = \left(0, 0, K \left(1 - \frac{\mu_2}{vr} \right), 0, 0 \right),$$

where the population size $S(t)$ of lead-free eagles grows to its carrying capacity $K \left(1 - \frac{\mu_2}{r} \right)$ and the population size $L(t)$ of eagles with subclinical lead toxicity grows to its carrying capacity $K \left(1 - \frac{\mu_2}{vr} \right)$. The equilibrium x_3^* corresponds to

the case where, in the absence of exposure to lead, subclinical lead toxicity persists through transmission of lead toxicity from mother to offspring ($L(t) > 0$). x_2^* must be such that $S^* > 0$. A necessary and sufficient condition is that births exceed deaths, that is, $r > \mu_2 > 0$. Likewise, x_3^* must be such that $L^* > 0$, which is satisfied when $vr > \mu_2$.

Solving for C^* , H^* , and T^* in terms of S^* and L^* in Eq. (16), (19) and (20), the equilibrium points for which $C^* > 0$ and $L^* > 0$ are

$$C^* = \frac{\Lambda}{\frac{\delta_1}{M}S^* + \frac{w\delta_1}{M}L^* + \mu_1}, \quad (31)$$

$$H^* = \frac{\frac{\omega_2}{M}\Lambda}{\sigma_1} \left(\frac{L^*}{\frac{\delta_1}{M}S^* + \frac{w\delta_1}{M}L^* + \mu_1} \right), \quad (32)$$

$$T^* = \frac{\eta \frac{\omega_2}{M}\Lambda}{\sigma_1\sigma_2} \left(\frac{L^*}{\frac{\delta_1}{M}S^* + \frac{w\delta_1}{M}L^* + \mu_1} \right). \quad (33)$$

Substituting $S^* = 0$ and Eq. (31), (32), and (33) into Eq. (18), L^* is solution to

$$c_0L^{*2} + c_1L^* + c_2 = 0, \quad (34)$$

where

$$c_0 = vr \frac{w\delta_1}{M} \sigma_1 \sigma_2, \quad (35)$$

$$c_1 = vr \left(\left(\mu_1 - \frac{w\delta_1}{M}K \right) \sigma_1 \sigma_2 + \frac{\omega_2}{M} \sigma_2 \Lambda + \eta \frac{\omega_2}{M}\Lambda \right) + \mu_2 \frac{w\delta_1}{M}K \sigma_1 \sigma_2, \quad (36)$$

$$c_2 = K \sigma_1 \sigma_2 \mu_1 \mu_2 + \frac{\omega_2}{M}\Lambda K (\sigma_1 \sigma_2 - \rho\eta) - vr\mu_1 K \sigma_1 \sigma_2. \quad (37)$$

If Eq. (34) has nonzero real roots L_4^* and L_5^* (with $L_4^* \geq L_5^*$, say), these roots lead to the two new equilibria:

$$x_4^* = (C_4^*, 0, L_4^*, H_4^*, T_4^*) \quad \text{and} \quad x_5^* = (C_5^*, 0, L_5^*, H_5^*, T_5^*), \quad (38)$$

where

$$C_4^* = \frac{\Lambda}{\frac{w\delta_1}{M}L_4^* + \mu_1}, \quad H_4^* = \frac{\frac{\omega_2}{M}\Lambda}{\sigma_1} \left(\frac{L_4^*}{\frac{w\delta_1}{M}L_4^* + \mu_1} \right), \quad \text{and}$$

$$T_4^* = \frac{\eta \frac{\omega_2}{M}\Lambda}{\sigma_1\sigma_2} \left(\frac{L_4^*}{\frac{w\delta_1}{M}L_4^* + \mu_1} \right),$$

and

$$C_5^* = \frac{\Lambda}{\frac{w\delta_1}{M}L_5^* + \mu_1}, \quad H_5^* = \frac{\frac{\omega_2}{M}\Lambda}{\sigma_1} \left(\frac{L_5^*}{\frac{w\delta_1}{M}L_5^* + \mu_1} \right), \quad \text{and}$$

$$T_5^* = \frac{\eta \frac{\omega_2}{M}\Lambda}{\sigma_1\sigma_2} \left(\frac{L_5^*}{\frac{w\delta_1}{M}L_5^* + \mu_1} \right).$$

Because $c_0 > 0$, Eq. (34) has real roots with opposite signs if and only if $c_2 < 0$. This corresponds to the case of a single additional equilibrium point, x_4^* , which is located in the first orthant. The condition $c_2 < 0$ is equivalent to

$$\frac{\omega_2}{M}\Lambda \left(1 - \frac{\rho\eta}{\sigma_1\sigma_2} \right) < \mu_1(vr - \mu_2), \quad (39)$$

which is satisfied if and only if,

$$\mu_1 > \frac{\frac{\omega_2}{M}\Lambda \left(1 - \frac{\rho\eta}{\sigma_1\sigma_2} \right)}{(vr - \mu_2)}, \quad (40)$$

because $\sigma_1\sigma_2 = (\eta + (\mu_2 + \mu_3))(\rho + (\mu_2 + \mu_4)) > \rho\eta$. Eq. (40) means that the smaller equilibrium for the total number of eagles with subclinical lead toxicity, L_5^* , is negative if the contaminated carrion decays quickly enough. The limiting case $c_2 = 0$ makes $L_1^* = 0$ and $x_4^* = x_1^*$.

On the other hand, Eq. (34) has two distinct real positive roots if and only if $c_2 > 0$, $c_1 < 0$, and $c_1^2 > 4c_0c_2$.

Because we assume that $vr > \mu_2$, it follows that $c_1 < 0$ is equivalent to the lower bound for the carrying capacity K :

$$K > \frac{vr(\mu_1\sigma_1\sigma_2 + \frac{\omega_2}{M}\sigma_2\Lambda + \eta \frac{\omega_2}{M}\Lambda)}{\frac{w\delta_1}{M}\sigma_1\sigma_2(vr - \mu_2)}. \quad (41)$$

The condition $c_2 > 0$ in Eq. (40) is equivalent to

$$\mu_1 < \frac{\frac{\omega_2}{M}\Lambda \left(1 - \frac{\rho\eta}{\sigma_2\sigma_2} \right)}{(vr - \mu_2)}. \quad (42)$$

Lastly, the condition $c_1^2 > 4c_0c_2$ is

$$\psi_1 > \psi_2, \quad (43)$$

where

$$\psi_1 = \left(vr(\mu_1 \frac{w\delta_1}{M} K\sigma_1\sigma_2 + \frac{\omega_2}{M}\sigma_2\Lambda + \eta \frac{\omega_2}{M}\Lambda) - (vr - \mu_2) \frac{w\delta_1}{M} K\sigma_1\sigma_2 \right)^2, \quad (44)$$

and

$$\psi_2 = 4Kvr \frac{w\delta_1}{M} \sigma_1 \sigma_2 \left(\frac{\omega_2}{M} \Lambda (\sigma_1 \sigma_2 - \rho \eta) - \sigma_1 \sigma_2 \mu_1 (vr - \mu_2) \right), \quad (45)$$

or equivalently,

$$\gamma_1 > \gamma_2, \quad (46)$$

where

$$\begin{aligned} \gamma_1 &= \frac{vrK^2}{M^2} \left((\mu_1 w\delta_1 \sigma_1 \sigma_2 + \omega_2 \Lambda (\sigma_2 + \eta) \omega_2 \Lambda)^2 + \left((1 - \frac{\mu_2}{vr}) w\delta_1 \sigma_1 \sigma_2 \right)^2 \right) \\ &\quad + 4K \frac{w\delta_1}{M} \sigma_1^2 \sigma_2^2 \mu_1 (vr - \mu_2), \end{aligned} \quad (47)$$

$$\begin{aligned} \gamma_2 &= 2 \left(\mu_1 \frac{w\delta_1}{M} K \sigma_1 \sigma_2 + \frac{\omega_2}{M} \sigma_2 \Lambda + \eta \frac{\omega_2}{M} \Lambda \right) (vr - \mu_2) \frac{w\delta_1}{M} K \sigma_1 \sigma_2 \\ &\quad + 4K \frac{w\delta_1}{M} \sigma_1 \sigma_2 \frac{\omega_2}{M} \Lambda (\sigma_1 \sigma_2 - \rho \eta). \end{aligned} \quad (48)$$

In sum, if the conditions in Eq. (41) and (42) hold with Eq. (43) or (46), then the two equilibria x_4^* and x_5^* exist and are distinct of one another.

To find equilibrium points in the positive orthant of \mathbb{R}^5 , we substitute Eq. (31), (32), and (33) into Eq. (17) to obtain the relation between S^* and L^* :

$$\begin{aligned} \sigma_2 \left(\sigma_1 \left(r \left(\frac{\delta_1}{M} S^* + \frac{w\delta_1}{M} L^* + \mu_1 \right) (K - L^* - S^*) - K \left(\mu_2 \frac{w\delta_1}{M} L^* + \mu_2 \frac{\delta_1}{M} S^* \right. \right. \right. \\ \left. \left. \left. + \Lambda \frac{\omega_1}{M} + \mu_1 \mu_2 \right) \right) - \frac{\omega_2}{M} r \Lambda L^* \right) - r \eta \Lambda \frac{\omega_2}{M} L^* = 0. \end{aligned} \quad (49)$$

Combining Eq. (17) multiplied by v with Eq. (49), we obtain the expression of S^* in terms of L^* at any equilibrium point where $S^* \neq 0$, taking the value:

$$S_6^* = \frac{\Gamma}{\sigma_1 \sigma_2 \left((1 - v) \frac{\delta_1}{M} \mu_2 L^* - \frac{\omega_1}{M} \Lambda \right)}, \quad (50)$$

where

$$\begin{aligned} \Gamma &= \sigma_1 \sigma_2 \frac{w\delta_1}{M} \mu_2 (1 - v) (L^*)^2 \\ &\quad + \left(\sigma_1 \sigma_2 \left(\left(\frac{\omega_2}{M} - v \frac{\omega_1}{M} \right) \Lambda + \mu_1 \mu_2 (1 - v) \right) - \eta \frac{\omega_2}{M} \rho \Lambda \right) L^*, \end{aligned} \quad (51)$$

Substituting Eq. (31), (32), (33), and (50) into Eq. (18) at any equilibrium point with $S^* \neq 0$ and $L^* \neq 0$ yields

$$b_0 L^{*3} + b_1 L^{*2} + b_2 L^* + b_3 = 0, \quad (52)$$

where

$$\begin{aligned}
b_0 = & -r\mu_2(\nu-1)\sigma_2\sigma_1 \\
& \times \left(\left(\left(\left(-\sigma_1 + (-\nu+1)\mu_2 \right) \frac{\omega_2}{M} + \frac{\omega_1}{M} \nu \sigma_1 \right) \sigma_2 \right) - \eta \left((\nu-1)\mu_2 - \rho \right) \frac{\omega_2}{M} \right) \frac{\delta_1}{M}^2 \\
& - \left(\sigma_1 \left(-\frac{\omega_2}{M} + \frac{\omega_1}{M}(\nu+1) \right) \sigma_2 + \frac{\omega_2}{M} \eta \rho \right) \frac{w\delta_1}{M} \frac{\delta_1}{M} + \frac{\omega_1}{M} \sigma_1 \sigma_2 \frac{w\delta_1}{M}^2 \right), \quad (53)
\end{aligned}$$

$$\begin{aligned}
b_1 = & \sigma_2^2 \sigma_1^2 \left(\mu_2 \left((\nu \frac{\omega_1}{M} - \frac{\omega_2}{M}) r - \mu_2 \left(\frac{\omega_1}{M} - \frac{\omega_2}{M} \right) \right) (\nu-1) K \frac{\delta_1}{M}^2 \right. \\
& + \left(\left(- \left(K \frac{w\delta_1}{M} - \nu \mu_1 - \mu_1 \right) \frac{\omega_1}{M} + \frac{\omega_2}{M} \mu_1 \right) (\nu-1) \mu_2 + \left((\nu-1) \frac{\omega_1}{M} - \frac{\omega_2}{M} \right) \Lambda \right. \\
& \left(\nu \frac{\omega_1}{M} - \frac{\omega_2}{M} \right) r + K \frac{w\delta_1}{M} \frac{\omega_1}{M} \mu_2^2 (\nu-1) \frac{\delta_1}{M} - \left(2 \mu_1 (\nu-1) \mu_2 + \left((\nu-1) \frac{\omega_1}{M} \right. \right. \\
& \left. \left. - \frac{\omega_2}{M} \right) \Lambda \right) r \frac{w\delta_1}{M} \frac{\omega_1}{M} + \Lambda \eta^2 r \rho^2 \frac{\omega_2}{M} \frac{\delta_1}{M} + \sigma_1 \sigma_2 \left(2 \frac{\delta_1}{M} \frac{\omega_1}{M} r \Lambda \mu_2 (\nu-1) \sigma_2 + \eta \left(K \rho \mu_2 \right. \right. \\
& \times (\nu-1) (r - \mu_2) \left(\frac{\delta_1}{M} \right)^2 + 2 \frac{\omega_2}{M} \left((\nu-1) \left(\frac{\omega_1}{M} \Lambda + \rho \frac{\mu_1}{2} \right) \mu_2 + \left((\nu - \frac{1}{2}) \frac{\omega_1}{M} - \frac{\omega_2}{M} \right) \right. \\
& \left. \left. \times \Lambda \rho \right) r \frac{\delta_1}{M} - \frac{w\delta_1}{M} \frac{\omega_1}{M} r \rho \Lambda \right), \quad (54)
\end{aligned}$$

$$\begin{aligned}
b_2 = & \left(\left(\sigma_1 \left(\left(\left(\nu \frac{\omega_1}{M} - \frac{\omega_2}{M} \right) \frac{\delta_1}{M} - \frac{w\delta_1}{M} \frac{\omega_1}{M} \right) K - \left((\nu-1) \frac{\omega_1}{M} - \frac{\omega_2}{M} \right) \mu_1 \right) r + \mu_2 K \right. \right. \\
& \left(\left((\nu-2) \frac{\omega_1}{M} + \frac{\omega_2}{M} \right) \frac{\delta_1}{M} + \frac{w\delta_1}{M} \frac{\omega_1}{M} \right) \Lambda - \mu_2 \mu_1 \left(\left(K \frac{\delta_1}{M} + \mu_1 \right) r - K \frac{\delta_1}{M} \mu_2 \right) \\
& \left. \left(\nu-1 \right) + \frac{\omega_1 \omega_2}{M} r \Lambda^2 \right) \sigma_2 + \left(\Lambda r \frac{\omega_1}{M} + \rho \left(\left(K \frac{\delta_1}{M} - \mu_1 \right) r - K \frac{\delta_1}{M} \mu_2 \right) \right) \\
& \Lambda \eta \frac{\omega_2}{M} \sigma_2 \sigma_1 \frac{\omega_1}{M}, \quad (55)
\end{aligned}$$

and

$$b_3 = \Lambda \left(\Lambda \frac{\omega_1}{M} - \mu_1 (r - \mu_2) \right) \frac{\omega_1}{M}^2 \sigma_2^2 \sigma_1^2 K. \quad (56)$$

We thus have found the equilibrium points with $S^* \neq 0$ given by Eq. (50) and L^* as a root of Eq. (52). This could, in principle, lead to three additional equilibrium points. However, the computation shows that two roots of the cubic of Eq. (52) are complex conjugates so that there is a single real solution L^* that, together with Eq. (50), leads to the last equilibrium:

$$x_6^* = (C_6^*, S_6^*, L_6^*, H_6^*, T_6^*), \quad (57)$$

where

$$C_6^* = \frac{\Lambda}{\frac{\delta_1}{M} S^* + \frac{w\delta_1}{M} L^* + \mu_1}, \quad H_6^* = \frac{\frac{\omega_2}{M} \Lambda}{\sigma_1} \left(\frac{L^*}{\frac{\delta_1}{M}} S^* + \frac{w\delta_1}{M} L^* + \mu_1 \right),$$

and

$$T_6^* = \frac{\eta \omega_2 \Lambda}{M \sigma_1 \sigma_2} \left(\frac{L^*}{\frac{\delta_1}{M} S^* + \frac{w\delta_1}{M} L^* + \mu_1} \right). \quad (58)$$

We have seen that all the coordinates of x_4^* in Eq. (38) are positive if $L_1^* > 0$, except for $S^* = 0$. Likewise, all coordinates of x_5^* are positive if $L_2^* > 0$, except for $S^* = 0$.

The equilibrium x_6^* is biologically relevant as long as $S^* > 0$ and $L^* > 0$. The complicated coefficients of Eq. (52) prevent us from deriving the algebraic constraints implying the existence of x_6^* with positive coordinates. We must be content with simulations to prove its existence.

3.4. Local stability of steady states

The Jacobian matrix is

$$J(x^*) = \begin{pmatrix} -L^* \frac{w\delta_1}{M} - S^* \frac{\delta_1}{M} - \mu_1 & -\frac{\delta_1}{M} C^* & -\frac{w\delta_1}{M} C^* & 0 & 0 \\ -\frac{\omega_1}{M} S^* & Y_1 & -\frac{rS^*}{K} & -\frac{rS^*}{K} & -\frac{rS^*}{K} \\ -\omega_2 M L^* + \frac{\omega_1}{M} S^* & \frac{\omega_1 K C^* - r v L^*}{K} & Y_2 & -\frac{r v L^*}{K} & \frac{-r v L^* + K \rho}{K} \\ \frac{\omega_2}{M} L^* & 0 & \frac{\omega_2}{M} C^* & -\sigma_1 & 0 \\ 0 & 0 & 0 & \eta & -\sigma_2 \end{pmatrix}, \quad (59)$$

where

$$\begin{aligned} Y_1 &:= \frac{r}{K} (K - N^* - S^*) - \left(\frac{\omega_1}{M} C^* + \mu_2 \right) \text{ and} \\ Y_2 &:= \frac{r v}{K} (K - N^* - L^*) - \left(\frac{\omega_2}{M} C^* + \mu_2 \right). \end{aligned} \quad (60)$$

The Jacobian evaluated at x_1^* is

$$J(x_1^*) = \begin{pmatrix} -\mu_1 & -\frac{\delta_1 \Lambda}{\mu_1} & -\frac{w\delta_1 \Lambda}{\mu_1} & 0 & 0 \\ 0 & \frac{(r - \mu_2)\mu_1 - \frac{\omega_1 \Lambda}{M}}{\mu_1} & 0 & 0 & 0 \\ 0 & \frac{\omega_1 \Lambda}{\mu_1} & \frac{(r v - \mu_2)\mu_1 - \omega_2 \Lambda}{\mu_1} & 0 & \rho \\ 0 & 0 & \frac{\omega_2 \Lambda}{\mu_1} & -\sigma_1 & 0 \\ 0 & 0 & 0 & \eta & -\sigma_2 \end{pmatrix}. \quad (61)$$

The first two diagonal coefficients are eigenvalues:

$$\lambda_1 = -\mu_1 < 0, \quad (62)$$

$$\lambda_2 = \frac{\mu_1(r - \mu_2) - \frac{\omega_1}{M} \Lambda}{\mu_1}, \quad (63)$$

which are both negative if and only if

$$r - \mu_2 < \frac{\frac{\omega_1}{M} \Lambda}{\mu_1}. \quad (64)$$

The remaining eigenvalues are the roots of the characteristic polynomial of the 3×3 remaining minor of $J(x_1^*)$, given by

$$-p_1(\lambda) = a_0\lambda^3 + a_1\lambda^2 + a_2\lambda + a_3, \quad (65)$$

where

$$a_0 = \mu_1, \quad (66)$$

$$a_1 = (\mu_2 - rv + \sigma_1 + \sigma_2)\mu_1 + \Lambda\omega_2, \quad (67)$$

$$a_2 = \mu_1\sigma_1\sigma_2 + (\sigma_1 + \sigma_2)(\mu_1(\mu_2 - rv) + \frac{\omega_2}{M}\Lambda), \quad (68)$$

$$a_3 = -\sigma_1\sigma_2(-\Lambda\omega_2 + \mu_1(rv - \mu_2)) - \Lambda\eta\rho\omega_2. \quad (69)$$

We use Routh's (1877) test to determine necessary and sufficient conditions for the stability of x_1^* . We need $a_i > 0$, $i = 0, 1, 2, 3$, and $a_1a_2 > a_0a_3$ to ensure that all the eigenvalues have negative real parts. $a_1 > 0$ if and only if

$$rv - \mu_2 < \sigma_1 + \sigma_2 + \frac{\frac{\omega_2}{M} \Lambda}{\mu_1}. \quad (70)$$

$a_2 > 0$ if and only if

$$rv - \mu_2 < \frac{\sigma_1\sigma_2}{\sigma_1 + \sigma_2} + \frac{\frac{\omega_2}{M} \Lambda}{\mu_1}, \quad (71)$$

which follows from Eq. (70), because $\sigma_1\sigma_2 \leq 4\sigma_1\sigma_2 \leq (\sigma_1 + \sigma_2)^2$. Finally, $a_3 > 0$ if and only if

$$rv - \mu_2 < \left(1 - \frac{\eta\rho}{\sigma_1\sigma_2}\right) \frac{\frac{\omega_2}{M} \Lambda}{\mu_1}, \quad (72)$$

which subsumes Eq. (70).

The last condition, $a_1a_2 > a_0a_3$, is equivalent to

$$\begin{aligned} & (\sigma_1 + \sigma_2)(\mu_1^2\sigma_1\sigma_2 + \mu_1\frac{\omega_2}{M}\Lambda) + \frac{\omega_2^2}{M}\Lambda^2(1 + \sigma_1 + \sigma_2) \\ & + \mu_1\frac{\omega_2}{M}\Lambda\rho\eta > (rv - \mu_2)\mu_1\frac{\omega_2}{M}\Lambda(1 + \sigma_1 + \sigma_2), \end{aligned} \quad (73)$$

that is,

$$r\nu - \mu_2 < \frac{\frac{\omega_2}{M}\Lambda}{\mu_1} + \frac{(\sigma_1 + \sigma_2)(\mu_1^2\sigma_1\sigma_2 + \mu_1\frac{\omega_2}{M}\Lambda) + \mu_1\frac{\omega_2}{M}\Lambda\rho\eta}{\mu_1\frac{\omega_2}{M}\Lambda(1 + \sigma_1 + \sigma_2)}. \quad (74)$$

This restriction is weaker than Eq. (72), which implies condition Eq. (73).

In summary, the equilibrium point x_1^* is locally asymptotically stable if

$$\frac{\frac{\omega_1}{M}\Lambda}{\mu_1} + \mu_2 < r < \left(1 - \frac{\eta\rho}{\sigma_1\sigma_2}\right) \frac{\frac{\omega_2}{M}\Lambda}{\nu\mu_1} + \frac{\mu_2}{\nu}. \quad (75)$$

This means that the per head birth rate r of lead-free eagles needs to belong to the interval

$$\left(\frac{\frac{\omega_1}{M}\Lambda}{\mu_1} + \mu_2, \left(1 - \frac{\eta\rho}{\sigma_1\sigma_2}\right) \frac{\frac{\omega_2}{M}\Lambda}{\nu\mu_1} + \frac{\mu_2}{\nu}\right), \quad (76)$$

which must be non-empty. A sufficient condition for this is, for example,

$$\nu < 1 - \frac{\eta\rho}{\sigma_1\sigma_2}, \quad (77)$$

which is $\nu < 0.8566$ using the parameter values displayed in Table 2. The corresponding range for r in order that x_1^* be locally asymptotically stable is approximately (426, 000, 428, 571), outside the realm of nature.

As for x_2^* , the Jacobian is

$$J(x_2^*) = \begin{pmatrix} \Theta_1 & 0 & 0 & 0 & 0 \\ -\frac{\omega_1 K(r-\mu_2)}{r} & \mu_2 - r & \mu_2 - r & \mu_2 - r & \mu_2 - r \\ \frac{\omega_1 K(r-\mu_2)}{r} & 0 & -\mu_2(1-\nu) & 0 & \rho \\ 0 & 0 & 0 & -\sigma_1 & 0 \\ 0 & 0 & 0 & \eta & -\sigma_2 \end{pmatrix}, \quad (78)$$

where

$$\Theta_1 := \left(-K\frac{\delta_1}{M} - \mu_1\right) + K\frac{\delta_1\mu_2}{Mr}. \quad (79)$$

Its eigenvalues are

$$\lambda_1 = -\sigma_2 < 0, \quad (80)$$

$$\lambda_2 = -\sigma_1 < 0, \quad (81)$$

Table 2. Lexicon of parameters.

Symbol	Description	Unit	Value (reference)
v	Fertility reduction of eagles with subclinical toxicity	1	0.70 (Gil-Sàncchez et al., 2018)
w	Consumption rate reduction of eagles with subclinical toxicity	1	0.90 (assumed)
M	Total mass of available carrion	kg	2.00×10^7 (Missouri Department of Conservation, 2012; Watt et al., 2012; Warner et al., 2014)
K	Carrying capacity of the Great Lakes region for bald eagles	1	4.60×10^3 (U.S. Fish and Wildlife Service, 2016)
λ	Rate of entry of contaminated carrion into the environment	kg/yr	3.00×10^6 (Freed and Yarbrough, 2008)
δ_1	Consumption rate for lead-free eagles	kg/yr	1.32×10^2 (National Eagle Center, 2020)
μ_1	Rate of decay for contaminated carrion	1/yr	1.00 (Jennelle et al., 2009)
μ_3	Mortality rate of eagles from clinical lead toxicity	1/yr	2.74 (Golden et al., 2016)
μ_4	Mortality rate from failure to treat lead toxicity	1/yr	0.22 (Strom et al., 2009)
μ_2	Mortality rate of eagles from other causes	1/yr	0.03 (National Eagle Center, 2020)
ω_1	For all carrion contaminated, subclinical lead-intoxication rate	1/yr	0.14 (Neumann, 2009)
ω_2	For all carrion contaminated, clinical lead-intoxication rate	1/yr	0.10 (Neumann, 2009)
r	Birth rate for lead-free eagles	1/yr	0.21 (U.S. Fish and Wildlife Service, 2016)
ρ	Rate of recovery from treatment	1/yr	1.00 (Redig et al., 2007a,b; Fallon et al., 2017)
η	Retrieval rate from clinical toxicity for treatment	1/yr	4.00 (variable; $0 \leq \eta < +\infty$)

$$\lambda_3 = \mu_2(v - 1) < 0, \quad (82)$$

$$\lambda_4 = \mu_2 - r < 0, \quad (83)$$

$$\lambda_5 = -\frac{\mu_1 + \frac{\delta_1}{M}K(r - \mu_2)}{r} < 0. \quad (84)$$

The equilibrium x_2^* is locally asymptotically stable. Likewise, for x_3^* ,

$$J(x_3^*) = \begin{pmatrix} \Theta_2 & 0 & 0 & 0 & 0 \\ 0 & \frac{\mu_2(1-v)}{v} & 0 & 0 & 0 \\ -\frac{\omega_2 K (rv - \mu_2)}{rv} & \mu_2 - rv & \mu_2 - rv & \mu_2 - rv & \mu_2 - rv + \rho \\ \frac{\omega_2 K (rv - \mu_2)}{rv} & 0 & 0 & -\sigma_1 & 0 \\ 0 & 0 & 0 & \eta & -\sigma_2 \end{pmatrix}, \quad (85)$$

where

$$\Theta_2 := \frac{K\mu_2 w \delta_1}{Mrv} - \left(K \frac{w \delta_1}{M} + \mu_1 \right). \quad (86)$$

with eigenvalues

$$\lambda_1 = -\sigma_2 < 0, \quad (87)$$

$$\lambda_2 = -\sigma_1 < 0, \quad (88)$$

$$\lambda_3 = -\frac{\mu_2(\nu - 1)}{\nu} > 0, \quad (89)$$

$$\lambda_4 = -(r\nu - \mu_2) < 0, \quad (90)$$

$$\lambda_5 = \frac{-\frac{w\delta_1}{M}K(r\nu - \mu_2) - r\nu\mu_1}{r\nu} < 0. \quad (91)$$

Because $\lambda_3 > 0$, x_3^* is an unstable equilibrium.

For the equilibria x_4^* , x_5^* , and x_6^* , determining the asymptotic stability analytically is more difficult. Our simulations performed with parameter values corresponding to bald eagles, show that x_4^* and x_5^* are unstable and x_6^* is locally asymptotically stable.

4. Simulations

We simulate the system to forecast the ecosystem made of carrion and bald eagles in the Great Lakes region at the 25-year horizon. We also assess the effects of the parameters for which there are no reliable estimates (ν , w , and μ_1) and of those depending on human intervention (rate Λ of entry of contaminated carrion and treatment rate η of eagles with clinical lead toxicity).

We modify Eq. (2), leading to the model:

$$C'(t) = \Lambda f(t) - \delta_1 \frac{C(t)}{M} S(t) - w\delta_1 \frac{C(t)}{M} L(t) - \mu_1 C(t), \quad (92)$$

$$S'(t) = rS(t) \left(1 - \frac{S(t) + L(t) + H(t) + T(t)}{K} \right) - \omega_1 \frac{C(t)}{M} S(t) - \mu_2 S(t), \quad (93)$$

$$L'(t) = \nu r L(t) \left(1 - \frac{S(t) + L(t) + H(t) + T(t)}{K} \right) + \omega_1 \frac{C(t)}{M} S(t) + \rho T(t) - \omega_2 \frac{C(t)}{M} L(t) - \mu_2 L(t), \quad (94)$$

$$H'(t) = \omega_2 \frac{C(t)}{M} L(t) - (\eta + \mu_2 + \mu_3) H(t), \quad (95)$$

$$T'(t) = \eta H(t) - (\rho + \mu_2 + \mu_4) T(t), \quad (96)$$

where the parameters are the same as in Eq. (2) to (6) and, for $n \in \mathbb{N}_0$,

$$f(t) = \begin{cases} 1, & n \leq t \leq n + 0.25, \\ 0, & n + 0.25 < t < n + 1. \end{cases} \quad (97)$$

In Eq. (97), the function f allows a switch reflecting the seasonality of the entry rate Λ of contaminated carrion. The annual big-game firearm hunting season takes place between the dates n in mid-October and $n + 0.25$ in mid-January.

To estimate the rate μ_1 of natural decay of carrion, we use Jennelle et al. (2009) who reported deer gut piles for 3 weeks to 3.5 months. We vary μ_1 within the range $[0, 24]$ year $^{-1}$, the upper limit corresponding to a mean presence of carrion of $\frac{1}{24}$ of a year, or 15 days and a half. We use the value $\mu_1 = 0$ to show the worst-case scenario in which the carrion does not decay but is entirely consumed by eagles.

Over the 25 years of the simulation, we find that the lead-free population is unaffected and that 1,430, or 20%, more eagles show subclinical toxicity for $\mu_1 = 0$ compared to $\mu_1 = 24$. This number is 830, or 12%, for $\mu_1 = 1$ compared to $\mu_1 = 24$.

After 25 years, when carrion is reduced from complete contamination to zero contamination, the total eagle population increases from 33,300 to 36,000, an 8.1% increase, and the total number of eagles with subclinical toxicity decreases from 13,700 to 7,300. In the more realistic case of reducing the current 15% contaminated carrion to 0, the effect on the total population after 25 years is an increase of 420 eagles (5.8%) accompanied by a decrease of 1,400 eagles with subclinical toxicity (-16%).

We vary the treatment rate η of eagles with clinical lead toxicity in the interval $[0, 100]$. After 25 years, the difference between $\eta = 0$ (never treated) and $\eta = 100$ (3.65 days from acquiring clinical toxicity to treatment) results in a 1% increase in the total population, or 35,400 for $\eta = 0$ and 35,760 for $\eta = 100$. Between $\eta = 1$, which corresponds to a delay of 1 year between acquiring clinical toxicity and treatment, and $\eta = 10$, corresponding to a delay of 5 weeks, the difference is only 30 birds, or 0.1%.

4.1. Sensitivity analysis

The sensitivity index ε of a state variable u with respect to a parameter p is

$$\varepsilon_p = \lim_{\delta p \rightarrow 0} \frac{\frac{\delta u}{|u|}}{\frac{\delta p}{|p|}} = \frac{|p|}{|u|} \frac{\partial u}{\partial p} = \frac{|p|}{|u|} u_p. \quad (98)$$

It is the percentage of change in the state variable corresponding to a 1% increase in the parameter.

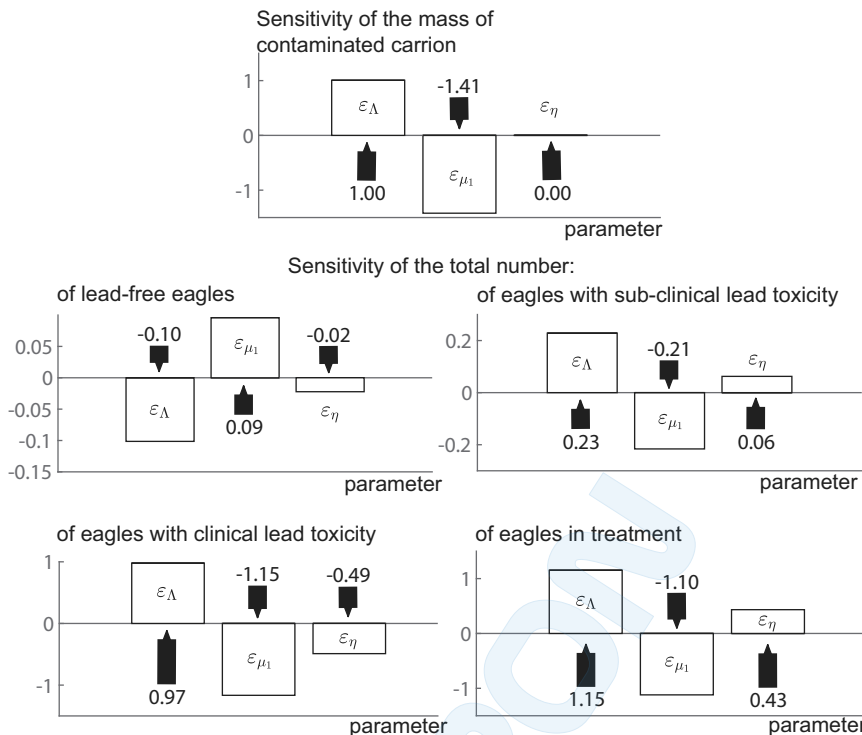


Figure 3. Sensitivity indices of the state variables with respect to the rate Λ of entry of contaminated carrion, the rate μ_1 of natural decay, and the rate η of retrieval for treatment at time $t = 25$ years.

4.1.1. The sensitivity of contaminated carrion

The mass C of contaminated carrion is highly sensitive to the entry rate Λ and to the rate μ_1 of natural decay of carrion, but not to the rate of retrieval η for treatment. Increasing Λ by 1% increases C by 1%. In contrast, a 1% increase in η results in a negligible effect on C . Increasing μ_1 by 1% makes the amount of contaminated carrion decrease by 1.41%.

4.1.2. Sensitivities of population sizes in each class

Increasing the rate Λ at which contaminated carrion enters the environment by 1% results in a decrease in the total number S of lead-free eagles by 0.1% after 25 years (Figure 3), because, lead-free eagles consume contaminated carrion and are intoxicated sooner. This is more consistent with the sensitivity of the total number L of eagles with subclinical lead toxicity with respect to Λ : Increasing Λ leads to more eagles with subclinical lead toxicity as more lead-free eagles get subclinical lead toxicity in the same amount of time, while eagles with subclinical lead toxicity, also consuming more contaminated carrion, take longer to develop clinical lead toxicity. To summarize, a 1% increase in the rate Λ of entry of contaminated carrion results in a 0.10% decrease in the total number S of lead-

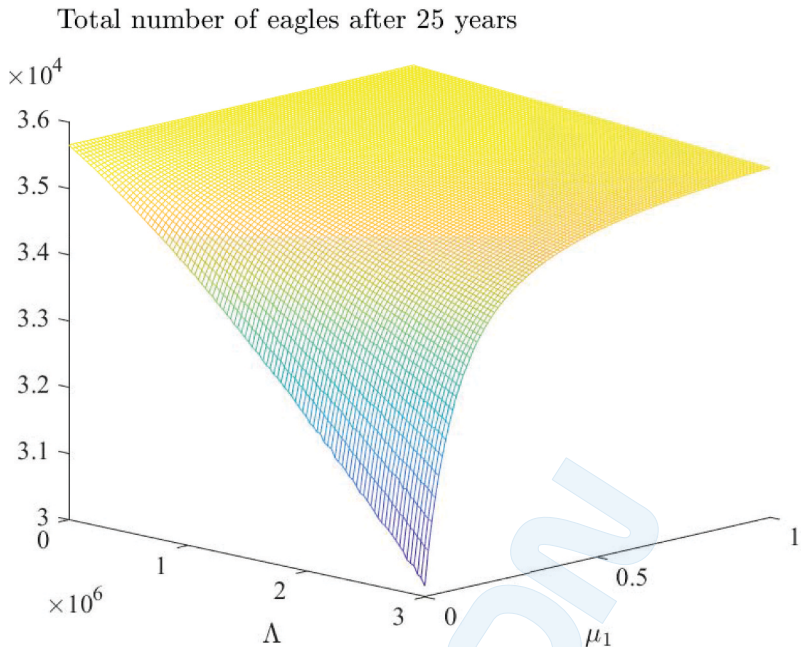


Figure 4. Total population size at time $t = 25$ years with respect to the rate Λ of entry of contaminated carrion and the rate μ_1 of natural decay.

free eagles, in a 0.23% increase in the total number L of eagles with subclinical lead toxicity, a 0.10% increase in the total number H of eagles with clinical lead toxicity, and a 1.15% increase in the total number T of eagles in treatment (Figure 4).

Figure 4 shows that a 1% increase in the rate μ_1 of natural decay causes a 0.1% increase in the total number S of lead-free eagles, a decrease in the total number L of eagles with subclinical lead toxicity by 0.2% and a decrease by 1.1% in the total number H of eagles with clinical lead toxicity and in the total number T of eagles in treatment. As the contaminated carrion decays faster, lead-free eagles eat less contaminated carrion, thus reducing the total number of eagles with subclinical lead toxicity who also eat less contaminated carrion. Even though eagles with clinical lead toxicity no longer consume carrion, their number decreases because fewer eagles with subclinical lead toxicity develop clinical lead toxicity. Decreasing the total number of eagles with clinical lead toxicity reduces the total number of eagles that need treatment for clinical lead toxicity.

An increase in the per head treatment rate η of eagles with clinical lead toxicity by 1% leads to a decrease in the total number S of lead-free eagles of 0.02%, a decrease in the total number H of eagles with clinical lead toxicity of 0.5%, an increase in the total number L of eagles with subclinical lead toxicity of 0.06%, and an increase in the total number T of eagles in treatment of 0.4% (Figure 3). This is consistent with the fact that treated eagles with clinical lead

toxicity never fully recover: They keep a subclinical lead toxicity; they will never be totally rid of lead. This explains both the decrease in the total numbers S of lead-free eagles and H of eagles with clinical lead toxicity and the increase in the total number L of eagles with subclinical lead toxicity.

Figure 4 shows the combined effect of varying the rate Λ of entry of contaminated carrion and the rate μ_1 of natural decay on the bald eagle population, where the height of the surface represents the total population size N of eagles.

The Water and Forestry Department could collect carrion, for example, thus increasing the rate of decay of carrion. However, at the current value of 3,000,000 kg/yr (at the front right edge of the surface in Figure 4), increasing the rate μ_1 of natural decay from its likely value in the range of 1–20 thousand tons per year for the rate Λ of entry of contaminated carrion has less effect than from a low value, such as 0.1–0.2, where the curve is steep. These values 0.1 to 0.2 correspond to a case when carrion keeps contaminating for 5 to 10 years, whereas empirically it only contaminates for several weeks to three months.

Even though the rate Λ of toxic entry could be forced down to 0 by law, it is seldom done because of its political cost, while increasing the rate μ_1 of natural decay of toxic substance is too expensive. Even without banning lead ammunition, reducing its use by two-thirds of the current value to 1,000 tons per year would increase the population size of eagles to 34,400 and make the action of μ_1 of secondary importance (the μ_1 -curve for the rate $\Lambda = 1$ of entry of contaminated carrion on the surface of Figure 4 is almost horizontal).

5. Conclusion

We have considered logistic growth for the subpopulation of lead-free eagles and for the one of eagles with subclinical lead toxicity as well as the mother-to-offspring transmission of lead toxicity. Usual epidemic models are inadequate because the lead toxicity is not contagious. We also considered the mass of contaminated carrion as responsible for the eagles' transition through the stages of the disease. The model describes vector or parasitic diseases for which the total vector or parasite population is not structured by disease stage, because the vector or parasite in this model is always infected. The vector therefore always occupies the same state "infected."

We simulated the consequences of the reduction in fertility, reduction in consumption, and acquisition of clinical lead toxicity, all due to chronic exposure to lead on the population of eagles.

We showed that the total population size depends much on the proportion of contaminated carrion but little on retrieval for treatment.

We considered deaths due to lead toxicity but ignored deaths due to injury resulting from the vulnerability induced by chronic lead toxicity, such as ocular and neurological lesions that affect flight ability and orientation (Neumann, 2009; Franson and Russell, 2014; Russell and Franson, 2014; Fallon et al., 2017).

We thus underestimate the damage caused by lead toxicity among bald eagles.

Eggshells harbor lead, and thus attest to mother-offspring transmission of lead to newborn eaglets (Burger, 1994; Vallverdú-Coll et al., 2015; Bruggeman et al., 2018). However, what is true for eggshells is not necessarily true for newborns. We could modify the model of Eq. (2) to (6) in this direction, with a probability that the eggshell represents the eaglet but at the cost of some complication.

We have found that the most effective way to reduce lead toxicity is to reduce the rate Λ of entry of contaminated carrion. This requires hunters to switch to lead-free ammunition. Copper ammunition is an alternative that may have little adverse effect in raptors, based on a laboratory study using kestrels as surrogates for raptors (Franson et al., 2011). A copper cartridge, in 2020 dollars, costs \$0.20 more than a lead cartridge. Because hunters fire a test round and allowing for two shots per animal hunted, this amounts to \$0.60 per deer hunted, for a total of \$540,000 for the 900,000 deer hunted per year. This cost is offset by savings in the capture and treatment of eagles with chronic lead toxicity. Even without this compensation, the projected increase in the eagle population of 2,700 eagles over 25 years amounts to \$5,000 per eagle, a very small price to pay for this natural treasure.

We also found that the population depends much on the rate μ_1 of natural decay of carrion, especially for large values of the rate Λ of entry of contaminated carrion. This means that increasing μ_1 by removing contaminated carrion is inefficient. This would work if the carrion decayed more slowly, as we showed by pushing the model out of the empirical values in Figure 4.

Disclosure statement

The authors report no potential conflict of interest.

Funding

The authors thank the National Science Foundation for award # 1757968, the National Security Agency for award # H98230-20-1-0164, and the Offices of the Provost and of the Dean of The College of Liberal Arts and Sciences at Arizona State University for funding this research.



References

American Eagle Foundation . (2020). Bald eagle diet. Retrieved January 7, 2020 from <https://www.eagles.org/what-we-do/educate/learn-about-eagles/bald-eagle-diet/>

Boyce, W. E. and DiPrima, R. C. (2005). *Elementary Differential Equations and Boundary Value Problems*. Somerset, NJ: Wiley.

Bruggeman, J. E., Route, W. T., Redig, P. T., et al. (2018). Patterns and trends in lead (Pb) concentrations in bald eagle (*Haliaeetus leucocephalus*) nestlings from the western Great Lakes region. *Ecotoxicology*, 27(5): 605–618. doi:[10.1007/s10646-0181933-5](https://doi.org/10.1007/s10646-0181933-5)

Bunnell, D. B., Barbiero, R. P., Ludsin, S. A., et al. (2013). Changing ecosystem dynamics in the Laurentian Great Lakes: bottom-up and top-down regulation. *BioScience*, 64(1): 26–39. doi:[10.1093/biosci/bit001](https://doi.org/10.1093/biosci/bit001)

Burger, J. (1994). Heavy metals in avian eggshells: another excretion method. *Journal of Toxicology and Environmental Health*, 41(2): 207–220. doi:[10.1080/15287399409531837](https://doi.org/10.1080/15287399409531837)

Cruz-Martinez, L., Redig, P. T., and Deen, J. (2012). Lead from spent ammunition: a source of exposure and poisoning in bald eagles. *Human-Wildlife Interactions*, 6(1): 94–104. doi:[10.2307/24874080](https://doi.org/10.2307/24874080)

Estes, J. A., Terborgh, J., Brashares, J. S., et al. (2011). Trophic downgrading of planet earth. *Science*, 33(6040): 301–306. doi:[10.1126/science.1205106](https://doi.org/10.1126/science.1205106)

Estes, J., Crooks, K., and Holt, R. D. (2001). Predators, Ecological Role of. In S. A. Levin (Ed.), *Encyclopedia of Biodiversity*. New York, NY: Elsevier, 857–878.

Fallon, J. A., Redig, P., Miller, T. A., et al. (2017). Guidelines for evaluation and treatment of lead poisoning of wild raptors. *Wildlife Society Bulletin*, 41(2): 205–211. doi:[10.1002/wsb.762](https://doi.org/10.1002/wsb.762)

Farquhar, B. (2020). *Wolf reintroduction changes ecosystem in Yellowstone*. Retrieved from July 1, 2020 <https://www.yellowstonepark.com/park/yellowstone-wolves-reintroduction>

Franson, J. C., Lahner, L. L., Meteyer, C., et al. (2011). Copper pellets simulating oral exposure to copper ammunition: absence of toxicity in American kestrels (*Falco sparverius*). *Archives of Environmental Contamination and Toxicology*, 62: 145–153. doi:[10.1007/s00244-011-9671-1](https://doi.org/10.1007/s00244-011-9671-1)

Franson, J. C. and Russell, R. E. (2014). Lead and eagles: demographic and pathological characteristics of poisoning, and exposure levels associated with other causes of mortality. *Ecotoxicology*, 23(9): 1722–1731. doi:[10.1007/s10646-014-1337-0](https://doi.org/10.1007/s10646-014-1337-0)

Freed, J. and Yarbrough, A. (2008). *Health Consultation: The Potential for Ingestion Exposure to Lead Fragments in Venison in Wisconsin*. Atlanta, Georgia: U.S. Dept. of Health and Human Services.

Gangoso, L., Alvarez-Lloret, P., Rodríguez-Navarro, A. A., et al. (2009). Long-term effects of lead poisoning on bone mineralization in vultures exposed to ammunition sources. *Environmental Pollution*, 157(2): 569–574. doi:[10.1016/j.envpol.2008.09.015](https://doi.org/10.1016/j.envpol.2008.09.015)

Gil-Sánchez, J. M., Molleda, S., Sánchez-Zapata, J. A., et al. (2018). From sport hunting to breeding success: patterns of lead ammunition ingestion and its effects on an endangered raptor. *Science of the Total Environment*, 613-614: 483–491. doi:[10.1016/j.scitotenv.2017.09.069](https://doi.org/10.1016/j.scitotenv.2017.09.069)

Golden, N. H., Warner, S. E., and Coffey, M. J. (2016). A review and assessment of spent lead ammunition and its exposure and effects to scavenging birds in the United States. In P. de Voogt (Ed.), *Reviews of Environmental Contamination and Toxicology* (Vol. 237). New York, NJ: Springer, 123–191. doi:[10.1007/978-3-319-23573-8_6](https://doi.org/10.1007/978-3-319-23573-8_6)

Hallam, T. G., Clark, C. E., and Jordan, G. S. (1983). Effects of toxicants on populations: a qualitative approach II. First order kinetics. *Journal of Mathematical Biology*, 18(1): 25–37. doi:[10.1007/BF00275908](https://doi.org/10.1007/BF00275908)

Harvey, C., Good, T., and Pearson, S. (2012). Top-down influence of resident and overwintering bald eagles (*Haliaeetus leucocephalus*) in a model marine ecosystem. *Canadian Journal of Zoology*, 90: 903–914. doi:[10.1139/Z2012-059](https://doi.org/10.1139/Z2012-059)

Hunt, H. W. (2012). Implications of sublethal lead exposure in avian scavengers. *Journal of Raptor Research*, 46(4): 389–393. doi:10.3356/JRR-11-85.1

Indiana Department of Natural Resources. (2020). Bald eagle. Retrieved July 15, 2020, from <https://www.in.gov/dnr/fishwild/3383.htm>

Jennelle, C. S., Samuel, M. D., Nolden, C. A., et al. (2009). Deer carcass decomposition and potential scavenger exposure to chronic wasting disease. *Journal of Wildlife Management*, 73 (5): 655–662. doi:10.2193/2008-282

Kramer, J. L. and Redig, P. T. (1997). Sixteen years of lead poisoning in eagles, 1980-1995: an epizootiologic view. *Journal of Raptor Research*, 31(4): 327–332.

Lindblom, R. A., Reichart, L. M., Mandernack, B. A., et al. (2017). Influence of snowfall on blood lead levels of free-flying bald eagles (*Haliaeetus leucocephalus*) in the upper Mississippi River valley. *Journal of Wildlife Diseases*, 53(4): 816–823. doi:10.7589/2017-02-027

Lodenius, M. and Solonen, T. (2013). The use of feathers of birds of prey as indicators of metal pollution. *Ecotoxicology*, 22(9): 1319–1334. doi:10.1007/s10646-013-1128-z

Magana, R., Dixon, A., Hakseth, C., et al. (2019). *Wisconsin bald eagle and osprey nest surveys 2019*. Madison: Wisconsin Department of Natural Resources. Retrieved July 1, 2020 from <https://dnr.wisconsin.gov/sites/default/files/topic/WildlifeHabitat/2019EagleOspreySurveys.pdf>

Maplesoft, a division of Waterloo Maple Inc. (2019). *Maple*. (Version 2019). Retrieved July 2, 2020 from <https://hadoop.apache.org>

Mathworks, Inc. (2019). *Matlab* (Version 9.6 (R2019a)).

Mathworks, Inc. (2020). *Matlab* (Version 9.8 (R2020a)).

Missouri Department of Conservation. (2012). *Deer harvest summary 2012-2013*. Retrieved July 15, 2020, from <https://huntfish.mdc.mo.gov/hunting-trapping/species/deer/deerharvest-reports/deer-harvest-summaries/deer-harvest-summary-2012>

National Eagle Center. (2020). *Eagle diet and feeding*. Retrieved July 15, 2020, from <https://www.nationaleaglecenter.org/eagle-diet-feeding/>

Neumann, K. (2009). Bald eagle lead poisoning in winter. In R. T. Watson, M. Fuller, M. Pokras, et al. (Eds.), *Ingestion of Lead from Spent Ammunition: Implications for Wildlife and Humans*, Boise. Boise, Idaho: The Peregrine Fund, 210–218.

Nixon, C. M., Hansen, L. P., Brewer, P. A., et al. (2001). Survival of white-tailed deer in intensively farmed areas of IL. *Canadian Journal of Zoology*, 79(4): 581–588. doi:10.1139/z01-010

R Core Team. (2019). *R: a language and environment for statistical computing*. R foundation for statistical computing. Vienna, Austria. Retrieved July 2, 2020 from <http://www.Rproject.org/>

Redig, P. T., Arent, L., Lopes, H., et al. (2007a). Rehabilitation. In D. M. Bird, K. Bildstein, D. R. Barber, et al. (Eds.), *Raptor Research and Management Techniques* (2nd Edition, Chap. 23). Blaine, WA: Hancock House, 411–422.

Redig, P. T., Arent, L., Lopes, H., et al. (2007b). Toxicology. In D. M. Bird, K. Bildstein, D. R. Barber, et al. (Eds.), *Raptor Research and Management Techniques* (2nd Edition, Chap. 23). Blaine, WA: Hancock House, 411–422.

Routh, E. J. (1877). *A Treatise on the Stability of A Given State of Motion: Particularly Steady Motion*. London, England: Macmillan.

Russell, R. E. and Franson, J. C. (2014). Causes of mortality in eagles submitted to the national wildlife health center 1975-2013. *Wildlife Society Bulletin*, 38(4): 697–704. doi:10.1002/wsb.469

Shepherd, S. (2019). *Bald eagle (*Halieetus leucocephalus*) status in Iowa, 2019*. Boone: Iowa Department of Natural Resources. Retrieved July 2, 2020 from <https://www.iowadnr.gov/Portals/idnr/uploads/Wildlife>

Simon, K. L., Best, D. A., Sikarskie, J. G., et al. (2020). Sources of mortality in bald eagles in MI, 1986-2017. *Journal of Wildlife Management*, 84(3): 553–561. doi:10.1002/jwmg.21822

Stauber, E., Finch, N., Talcott, P. A., et al. (2010). Lead poisoning of bald (*Haliaeetus leucocephalus*) and golden (*Aquila chrysaetos*) eagles in the US inland Pacific northwest region-an 18-year retrospective study: 1991-2008. *Journal of Avian Medicine and Surgery*, 24 (4): 279-287. doi:10.1647/2009-006.1

Strom, S. M., Langenberg, J. A., Businga, N. K., et al. (2009). Lead exposure in Wisconsin birds. In R. T. Watson, M. Fuller, M. Pokras, et al. (Eds.), *Ingestion of Lead from Spent Ammunition: Implications for Wildlife and Humans*. Boise, ID: The Peregrine Fund, 194-201.

Suckling, K. and Hodges, W. (2007). Status of the bald eagle in the lower 48 states and the District of Columbia: 1963-2007. Center for Biological Diversity. Retrieved July 1, 2020 from <https://www.biologicaldiversity.org/species/birds/baldeagle/report/index.html>

U.S Fish and Wildlife Service Midwest Region. (2020a). *Bald eagle breeding pairs 1990 to 2006*. Retrieved July 1, 2020 from <https://www.fws.gov/midwest/eagle/NestingData/nosstatetbl.html>

U.S. Fish and Wildlife Service Midwest Region. (2020b). *Nest chronology of bald eagles in the midwest*. Retrieved July 2, 2020 from <https://www.fws.gov/midwest/eagle/Nhistory/NestChron.html#nesting>

U.S. Fish and Wildlife Service. (2016). *Bald and golden eagles: population demographics and estimation of sustainable take in the United States, 2016 update*. Division of Migratory Bird Management. Retrieved July 1, 2020 from <https://www.fws.gov/migratorybirds/pdf/management/EagleRuleRevisions-StatusReport.pdf>

Vallverdú-Coll, N., Lopez-Antia, A., Martinez-Haro, M., et al. (2015). Altered immune response in mallard ducklings exposed to lead through maternal transfer in the wild. *Environmental Pollution*, 205: 350-356. doi:10.1016/j.envpol.2015.06.014

Warner, S. E., Britton, E. E., Becker, D. N., et al. (2014). Bald eagle lead exposure in the upper midwest. *Journal of Fish and Wildlife Management*, 5(2): 208-216. doi:10.3996/032013-JFWM-029

Watt, M. A., Norton, A. S., Van Deelen, T. R., et al. (2012). *WI deer research studies, annual report 2011-2012*. Madison: Wisconsin Department of Natural Resources.

Wisconsin Department of Natural Resources. (2017). *2019 WI hunting and trapping seasons*. Madison: Wisconsin Department of Natural Resources. Retrieved July 1, 2020 from dnr.wi.gov

Wolfram Research, Inc. (2020). *Mathematica (Version 12.1)*. Retrieved July 2, 2020 from <https://www.wolfram.com/mathematica>

Woodford, J., Henry, J., Edlin, D., et al. (2017). *Wisconsin bald eagle and osprey nest surveys 2017*. Madison: Wisconsin Department of Natural Resources. Retrieved July 2, 2020 from <http://dnr.wi.gov/topic/wildlifehabitat/documents/reports/eagleospreysurv.pdf>

Yaw, T., Neumann, K., Bernard, L., et al. (2017). Lead poisoning in bald eagles admitted to wildlife rehabilitation facilities in IA, 2004-2014. *Journal of Fish and Wildlife Management*, 8 (2): 465-473. doi:10.3996/122015-JFWM-124